DEFENSE DOCUMENTATION CENTER

FOR

SCIENTIFIC AND TECHNICAL INFORMATION

CAMERON STATION, ALEXANDRIA, VIRGINIA

N-63-4-2

THERMAL DIFFUSION OF VACANCIES IN ZINC

by

W. C. OLANDER

R. A. SWALIN

DEPARTMENT OF METALLURGY

INSTITUTE OF TECHNOLOGY

UNIVERSITY OF MINNESOTA
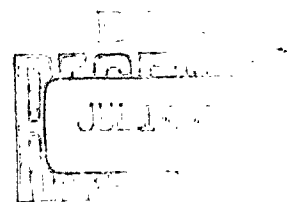
THERMAL DIFFUSION OF VACANCIES IN ZINC

by

W. C. Olander*

and

R. A. Swalin**

Fifth Technical Report

June 1, 1963

Contract Nonr 710(27)

*Formerly with the Department of Metallurgy, University of Minnesota; now with A.C. Sparkplug Division, El Segundo, California.

**Professor and Head, Department of Metallurgy, University of Minnesota, Minneapolis, Minnesota.

Department of Metallurgy
University of Minnesota
Minneapolis 14, Minnesota

June 1, 1963

Metallurgy Branch (Code 423)
Office of Naval Research
Department of Navy
Washington 25, D. C.

Gentlemen:

This technical report entitled "Thermal Diffusion
of Vacancies in Zinc" was prepared under contract
Nonr 710(27) and represents the fifth technical report
dealing with the general subject of point defects in
crystalline solids. The essential findings are summarized
briefly in the next page.

We appreciate the support for our work provided by
the Office of Naval Research.

Sincerely yours,

Richard A. Swalin
Professor and Head

RAS:jm

ABSTRACT

Thermal Diffusion of Vacancies in Zinc

An apparatus has been constructed which yields a nearly linear temperature gradient for pure metal samples. Thermal diffusion of vacancies in pure zinc has been studied by use of a surface marker motion technique. Results compiled to date indicate that marker movement does exist when a temperature gradient is applied to a pure zinc crystal. Preliminary calculations of the total energy term associated with the flux equation yield a value of approximately -8.8 k cal/mole. In the future it is planned to investigate more thoroughly the role of surface tension in causing shape changes and thermal diffusion will be studied by the use of inert markers embedded in the sample.

TABLE OF CONTENTS

THERMAL DIFFUSION OF VACANCIES IN ZINC

I. Introduction

When a temperature gradient is impressed upon an initially
homogeneous multicomponent system, an unmixing of the components of
this system may take place and this occurrence is called the Ludwig-
Soret effect or thermal diffusion.

In terms of the formality of irreversible thermodynamics of
Denbigh[1], a temperature gradient is a secondary driving force for
diffusion, the primary and most commonly considered driving force
is that of a chemical potential gradient. Since crystal defects,
(vacancies in particular) are components of a metal system it is
predicted that these will flow as a direct result of the application
of a temperature gradient and indirectly through the influence of a
gradient of local equilibrium concentration due to the temperature
dependence. It is assumed that the rates of creation and annihila-
tion of defects are high enough at each point to maintain a local
concentration corresponding to isothermal equilibrium at the local
temperature. It is hypothesized that dislocations act sufficiently
well as vacancy sources and sinks to insure the local isothermal
equilibrium concentration of vacancies. Under the conditions of a
temperature gradient coupled with the assumption of a local equilib-
rium concentration of vacancies at each point in the crystal a
continuous flow of vacancies may occur.

Phenomenologically the equations of irreversible thermodynamics
predict a redistribution of initially homogeneous components in a

temperature gradient so as to produce entropy or to transport heat down the temperature gradient. A measure of how strongly a component will be driven toward the hot or cold direction is given by the heat of transport of the component, Q_i^*. The heat of transport represents the apparent amount of heat carried by an atom.

Thermal diffusion has been measured in gases, liquids and solids (2-10). Several attempts to observe the thermal diffusion of vacancies in a pure metal have been made (11-13) and only Meechan and Lehman[13] using an extremely steep gradient have been successful in observing marker motion. Several treatments of the theoretical aspects of thermal diffusion, both phenomenological and atomistic, have appeared in the references listed above and also in several other references (14-24).

A study of thermal diffusion in metals is important for two reasons. Technologically it is important because as operating temperatures of materials become higher, thermal diffusion due to temperature gradients existing in these materials serves to transport defects and atomic constituents. This transport may change the mechanical, electrical, or chemical properties of the material over a period of time and may result in a deterioration of desirable qualities.

In a more basic sense the study of thermal diffusion leads to a consideration of the details of the mechanism of diffusion in metals and may give detailed information concerning the nature of the activated state.

Relatively little experimental thermal diffusion work has been done to date in solids. One of the important reasons for this is that the experimental techniques are quite difficult. In addition, many serious questions may arise such as to the quantity which is actually being measured and the nature of the temperature gradient along the specimen.

The theoretical problem of thermal diffusion may be treated by the kinetic consideration of the steady state in a temperature gradient or by the utilization of thermodynamics of irreversible processes. Wirtz[14] develops a general kinetic theory which Shockley[16,19] Brinkman[18], and LeClaire[17] apply to the case of self diffusion in solids. Shewmon[11] makes use of the thermodynamic approach and applies this to the case of thermal diffusion of vacancies in zinc. Allnatt and Rice[21] also present a thermodynamic approach to thermal diffusion. Both the kinetic and thermodynamic approaches lead to an expression for the net atom current density J given by Meechan and Lehman[13] as

$$J = \frac{D}{kT^2\lambda} \frac{dT}{dy} (\Delta E) \tag{1}$$

where D is the self diffusion coefficient, λ is the lattice spacing, T is the absolute temperature, k is Boltzmann's constant, $\frac{dT}{dy}$ is the temperature gradient, and ΔE is an energy term which characterizes the algebraic sum of various energy considerations included in the system and may be positive or negative for a given system. The difference between the kinetic and thermodynamic approaches is in the derivation and interpretation of ΔE

as is stated by Meechan and Lehman.

One interpretation of the observation of lack of thermal diffusion of vacancies by Shewmon[11] in zinc and by Brammer (12,25) in α iron and copper is given by these investigators as meaning that perhaps the ΔE term in Equation 1 above is zero.

It should be pointed out that other considerations regarding the experiments themselves might be important and that thermal diffusion of vacancies in these materials mentioned above quite possibly did occur but was not observed due to particular circumstances of the experiment. This point will be discussed later in more detail.

The usual way in which thermal diffusion of vacancies experiments are conducted is to measure the relative motion between markers on a sample exposed to a temperature gradient and to relate this motion to the flux in Equation 1 and thus to ΔE.

The flux of vacancies past two markers at different positions along the temperature gradient could be the same due to some anomaly in the temperature gradient such as a broad minimum or maximum, or due to the fact that there is a maximum for some temperature gradient conditions in the J vs T curve of Equation 1. If the flux past the two markers due to one of these causes is the same, there will be no relative motion between the markers and this would be erroneously interpreted to mean that no thermal diffusion exists. This implies that detailed knowledge of the temperature profile encountered by the sample is extremely important with regard to the

successful interpretation of the marker motion of a thermal diffusion experiment. Also, when an extremely large temperature gradient is used, it is possible that a large portion of the sample is at such a low temperature that the fluxes themselves are very low and thus the difference between such low fluxes would not lead to relative marker movement which is observable in a reasonable period of time.

The thermal diffusion of vacancies in zinc has been chosen for experimental investigation for several reasons. Zinc has a relatively low melting point of 419.5°C. and is relatively easy to obtain in crystalline form with a purity of 99.99 per cent. Previously no thermal diffusion has been observed for vacancies in pure zinc[11] and this observation is quite puzzling from a theoretical point of view. As a result it seemed advisable to re-examine this system using apparatus which has closer control of the temperature gradient.

II. Theory

A. Phenomenological Theory

1. Derivation of Flux Equation

The phenomenological equations for the thermal diffusion of vacancies in a pure metal are derived using the irreversible thermodynamic formality of Davies[26]. The flux equation derived using this approach is very similar to that of Shewmon[11] who also used this macroscopic theory of irreversibility formality.

The phenomenological equations of motion are given by Davies[26] as

$$J_1 = L_{11}^* \left[-\frac{1}{T} (\delta \mu_1)_T + Q_1^* \delta (\tfrac{1}{T}) \right] + L_{12}^* \left[-\frac{1}{T} (\delta \mu_2)_T + Q_2^* \delta(\tfrac{1}{T}) \right] \quad (2)$$

$$J_2 = L_{21}^* \left[-\frac{1}{T} (\delta \mu_1)_T + Q_2^* \delta (\tfrac{1}{T}) \right] + L_{22}^* \left[-\frac{1}{T} (\delta \mu_2)_T + Q_2^* \delta(\tfrac{1}{T}) \right] \quad (3)$$

$$J_3^* = k \, \delta (\tfrac{1}{T}) + Q_1^* J_1 + Q_2^* J_2 \quad (4)$$

where subscripts 1, 2, 3 refer to metal atoms, vacancies and energy respectively. The J's represent fluxes, μ represents chemical potential, T is the absolute temperature, k is Boltzmann's constant and the L_{ij}^* are phenomenological coefficients. J_3^* represents an energy flow relative to an internal energy zero taken such that $J_3^* = J_E - \bar{h} J_m$ where J_E is the rate of change of internal energy, $\bar{h}$ is the average enthalpy and J_m is the mass flow. Q^* is defined by Davies as

$$Q_i^* = \sum_j (L_{ij}^*)^{-1} L_{j3}^* \quad (5)$$

In the present case this results in:

$$Q_1^* = \frac{L_{13}^*}{L_{11}^*} + \frac{L_{23}^*}{L_{12}^*} \quad \text{and} \tag{6}$$

$$Q_2^* = \frac{L_{13}^*}{L_{22}^*} + \frac{L_{23}^*}{L_{22}^*} \tag{7}$$

Account is now taken of the fact that the two components, metal atoms and vacancies, are related through

$$J_1 + J_2 = 0. \tag{8}$$

Thus

$$L_{11}^* + L_{21}^* = 0 \tag{9}$$

and

$$L_{11}^* = -L_{21}^*. \tag{10}$$

Also

$$L_{12}^* + L_{22}^* = 0 \tag{11}$$

results from Equation (8) and thus:

$$L_{12}^* + L_{22}^* = 0 \tag{12}$$

Insertion of the Onsager relations $L_{ij}^* = L_{ji}^*$ yields the following relations:

$$L_{11}^* = L_{22}^* = -L_{12}^* \tag{13}$$

Equations (6) and (7) combined with Equation (13) result in:

$$Q_1^* = \frac{L_{13}^* - L_{23}^*}{L_{22}^*} \tag{14}$$

and

$$Q_2^* = \frac{L_{23}^* - L_{13}^*}{L_{22}^*} \tag{15}$$

The relationship between Q_1^* and Q_2^* follows naturally from Equations (14) and (15) and is

$$Q_1^* = -Q_2^* .\qquad (16)$$

The representation of δ is taken to be $\frac{d}{dy}$. The chemical potential of component 1, metal atoms, is given by

$$\mu_1 = \mu_1^\circ + kT \ln a_1 \qquad (17)$$

where a_1 is the activity of component 1. If a dilute solution of vacancies in the metal is assumed then the solute follows Henry's law and

$$a_2 = bN_2 \qquad (18)$$

where a_2 is the activity of the vacancies, b is a constant and N_2 is the mole fraction of vacancies. The activity of the solvent in a dilute solution is just equal to the mole fraction of the solvent:

$$a_1 = N_1 . \qquad (19)$$

Thus
$$(\delta\mu_1)_T = kT \frac{d\ln a_1}{dy} = kT \frac{d\ln N_1}{dy} \qquad (20)$$

or
$$(\delta\mu_1)_T = kT \frac{dT}{dy} \frac{d\ln N_1}{dT} . \qquad (21)$$

Similarly
$$(\delta\mu_2)_T = kT \frac{dT}{dy} \frac{d\ln N_2}{dT} \qquad (22)$$

and also
$$\delta(\frac{1}{T}) = -\frac{1}{T^2} \frac{dT}{dy} . \qquad (23)$$

Substituting Equations (21), (22), (23), and (13) in Equation (2):

$$J_1 = -L_{11}^* \left[k\frac{dT}{dy}\frac{d \ln N_1}{dT} + \frac{Q_1^*}{T^2}\frac{dT}{dy} - \frac{k}{dy}\frac{dT}{dy}\frac{d \ln N_2}{dT} - \frac{Q_2^*}{T^2}\frac{dT}{dy} \right] \quad (24)$$

or

$$J_1 = -\frac{L_{11}^*}{T^2}\frac{dT}{dy}\left[kT^2 (\frac{d \ln N_1}{dT} - \frac{d \ln N_2}{dT}) + Q_1^* - Q_2^* \right] \quad (25)$$

Introducing the mole fraction relation:

$$N_1 + N_2 = 1 \quad (26)$$

and

$$-dN_1 = dN_2 . \quad (27)$$

Then

$$\frac{d \ln N_1}{dT} = -\frac{N_2}{N_1}\frac{d \ln N_2}{dT} \quad (28)$$

and Equation (25) is transformed to

$$J_1 = -\frac{L_{11}^*}{T^2}\frac{dT}{dy}\left[-\frac{kT^2}{N_1}\frac{d \ln N_2}{dT} + Q_1^* - Q_2^* \right] \quad (29)$$

The temperature dependence of N_2 is

$$N_2 = A\exp\left(-\frac{\Delta Hv}{kT} \right) \quad (30)$$

where ΔHv is the heat of formation of vacancies and A is a constant. Taking the temperature derivative of Equation (30) and utilizing this result in Equation (29):

$$J_1 = -\frac{L_{11}^*}{T^2}\frac{dT}{dy}\left[Q_1^* - Q_2^* - \frac{\Delta H_v}{N_1} \right] \quad (31)$$

The insertion of Equation (16) in Equation (31) results in:

$$J_1 = -\frac{L_{11}^*}{T^2} \frac{dT}{dy} \left[2Q_1^* - \frac{\Delta Hv}{N_1} \right] \qquad (32)$$

The self diffusion coefficient D_1 is related to L_{11}^* through

$$L_{11}^* = \frac{C_1 D_1}{k} \qquad (33)$$

where C_1 is the concentration of metal atoms in atoms per unit volume. Thus

$$J_1 = -\frac{C_1 D_1}{kT^2} \frac{dT}{dy} \left[2Q_1^* - \frac{\Delta Hv}{N_1} \right] \qquad (34)$$

or

$$J_1 = -\frac{C_1 D_1}{kT^2} \frac{dT}{dy} \Delta E \qquad (35)$$

where

$$\Delta E = 2Q_1^* - \frac{\Delta Hv}{N_1} \qquad (36)$$

2. Relation of Flux to Relative Marker Movement and Energy Term ΔE.

If J_{T_1} is the flux of atoms at the marker at temperature T_1 and J_{T_2} is the flux of atoms at the marker at T_2 then $J_{T_1} - J_{T_2}$ represents the net flux into the region of crystal between the markers at T_1 and T_2. This term multiplied by the cross sectional area A of the sample results in the net flow rate of material entering the volume bounded by the markers at T_1 and T_2. The flow rate multiplied by the molar volume V equals the rate of increase in volume of the material between the markers. This rate of increase

of volume multiplied by the time between measurements of marker positions gives the increase in volume between the markers.

Thus

$$\Delta V = \left[J_{T_1} - J_{T_2} \right] VA\ t \tag{37}$$

If it is assumed that the cross-sectional area remains constant, $\Delta V = A\Delta x$ where Δx is the change in distance between the markers. Thus:

$$\Delta x = - \frac{t\ \Delta EV_1}{R}\ \frac{dT}{dy} \left[\frac{D_{T_1} C_{T_1}}{T_1^2} - \frac{D_{T_2} C_{T_2}}{T_2^2} \right] \tag{38}$$

Therefore:

$$\Delta E = - \frac{R\Delta x}{tv_1} \left[\frac{1}{\frac{dT}{dy}\left(\frac{D_{T_1} C_{T_1}}{T_1^2} - \frac{D_{T_2} C_{T_2}}{T_2^2} \right)} \right] \tag{39}$$

Measurement of the change in distance between markers as a function of time results in a measurement of the magnitude and size of the composite ΔE energy term.

Equation (39) may be simplified by noting that

$$V_1 C_1 = \frac{\text{volume component 1}}{\text{total volume}}$$

and this ratio is very close to one.

$$\Delta E \cong - \frac{R\Delta x}{t} \left[\frac{1}{\left(\frac{dT}{dy}\right)\left(\frac{D_{T_1}}{T_1^2} - \frac{D_{T_2}}{T_2^2} \right)} \right] \tag{40}$$

B. Marker Movement

Equation (35) of the proceeding section shows that J_1 is a function of temperature. The shape of the J_1 vs T curve and the relation of actual experimental conditions to this curve has implications regarding the relative marker movement in different parts of the sample.

The self diffusion coefficient of component 1

$$D_1 = D_o \exp(\frac{-\Delta H_D}{RT})$$

(41)

is substituted into Equation (35) giving

$$J_1 = \frac{D_o \exp\left(\frac{-\Delta H_D}{RT}\right)}{RT^2} \frac{dT}{dy} \Delta E$$

(42)

where D_o, ΔH_D, and ΔE, are all constants. At this point the discussion is limited to the consideration of linear temperature gradients; thus dT/dy is constant also. It is possible to express the above mentioned constants in terms of other constants, A and B to emphasize the fact that J_1 is a function of T. This operation results in

$$J_1 = \frac{A \exp (-B/T)}{T^2}$$

(43)

where A and B are constants and $\frac{\Delta H_D}{R} = B > 0$. A normalized version of Equation (43) is plotted in Fig. 1 which displays $B^2 J_1/A$ vs T. There is a maximum in this curve, and this means that although a linear temperature gradient may exist in the thermal diffusion sample it is possible to have equal fluxes at two

GENERAL RELATION - MASS FLUX vs TEMPERATURE

$$J = \frac{A\exp^{\left(-B/T\right)}}{T^2}$$

$\left(\frac{B^2}{A}\right) J$

Jv ↓
J_I ↑
Jm ↓
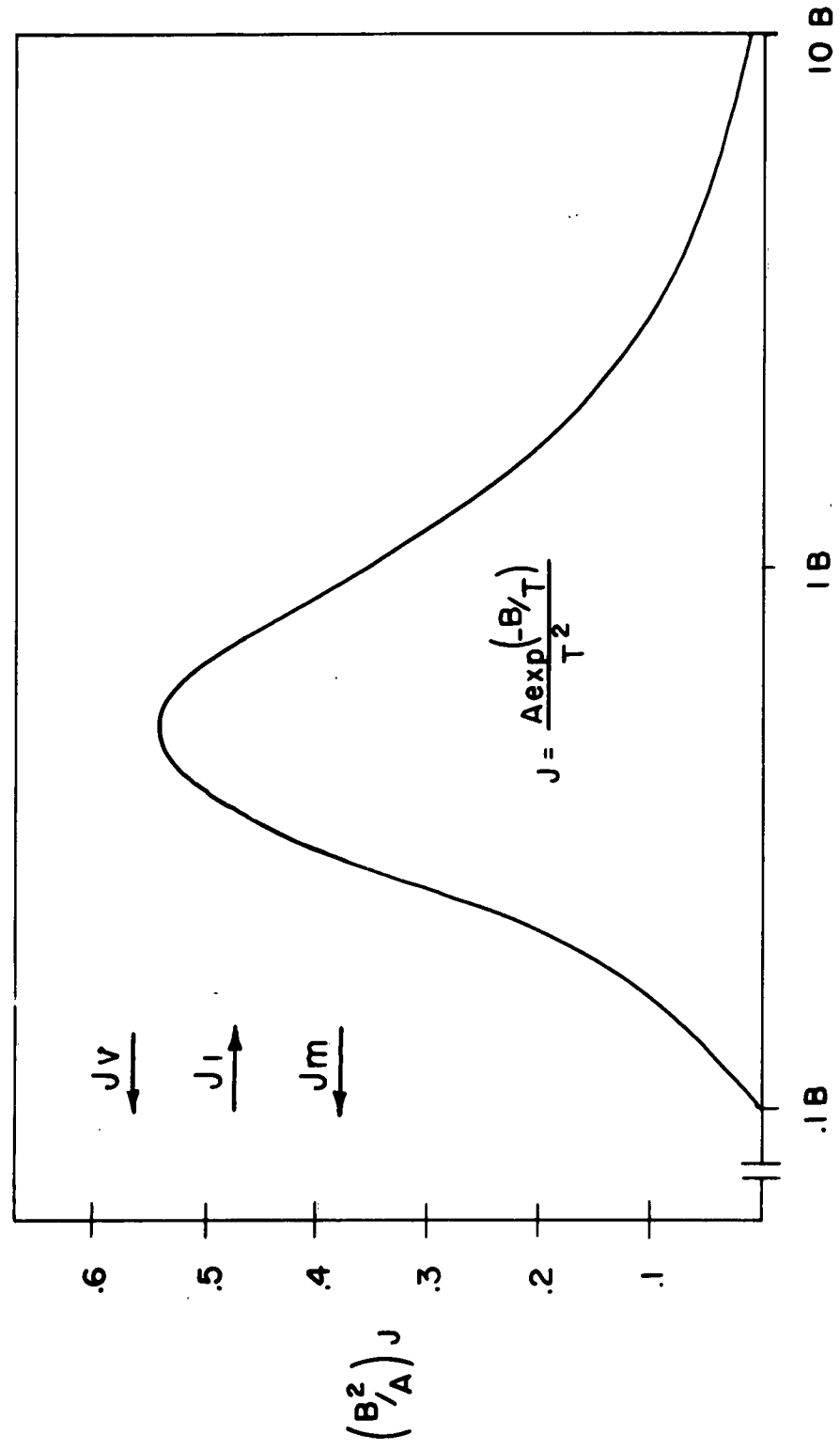
T ⟶

FIGURE 1

different points on the specimen. Since the direction of flow of metal atoms and markers in the specimen is dictated by the sign of the ΔE term included in constant A, it must be concluded that under conditions of a linear temperature gradient the atoms or markers may flow in one direction only.

The difference in flow rates past two markers depends upon the position of the markers relative to the maximum in the J_1 vs T curve. It is important to know just what the actual experimental conditions are relative to the J_1 vs T curve so that the relative marker displacement may be interpreted meaningfully. A typical plot of the experimental conditions existing for the work reported here is presented as Fig. 2, and this figure shows no maximum in the actual temperature range utilized experimentally.

If a region of sample exists between two marks such that the flux of vacancies into the region from one end is higher than the flux leaving the other end the distance between the marks must decrease because the net effect is to displace atoms from the region. Conversely if the flux of vacancies leaving one end of a region between two markers is higher than the flux entering the other end, the distance between markers bounding the region will increase. Fig. 2 predicts a contraction of the distances between all markers if the vacancies move toward the cold end of the sample and an expansion of the distances between markers if they move toward the hot end.

MASS FLUX vs TEMPERATURE

(TYPICAL EXPERIMENT)

SAMPLE LENGTH

(TEMPERATURE °K)
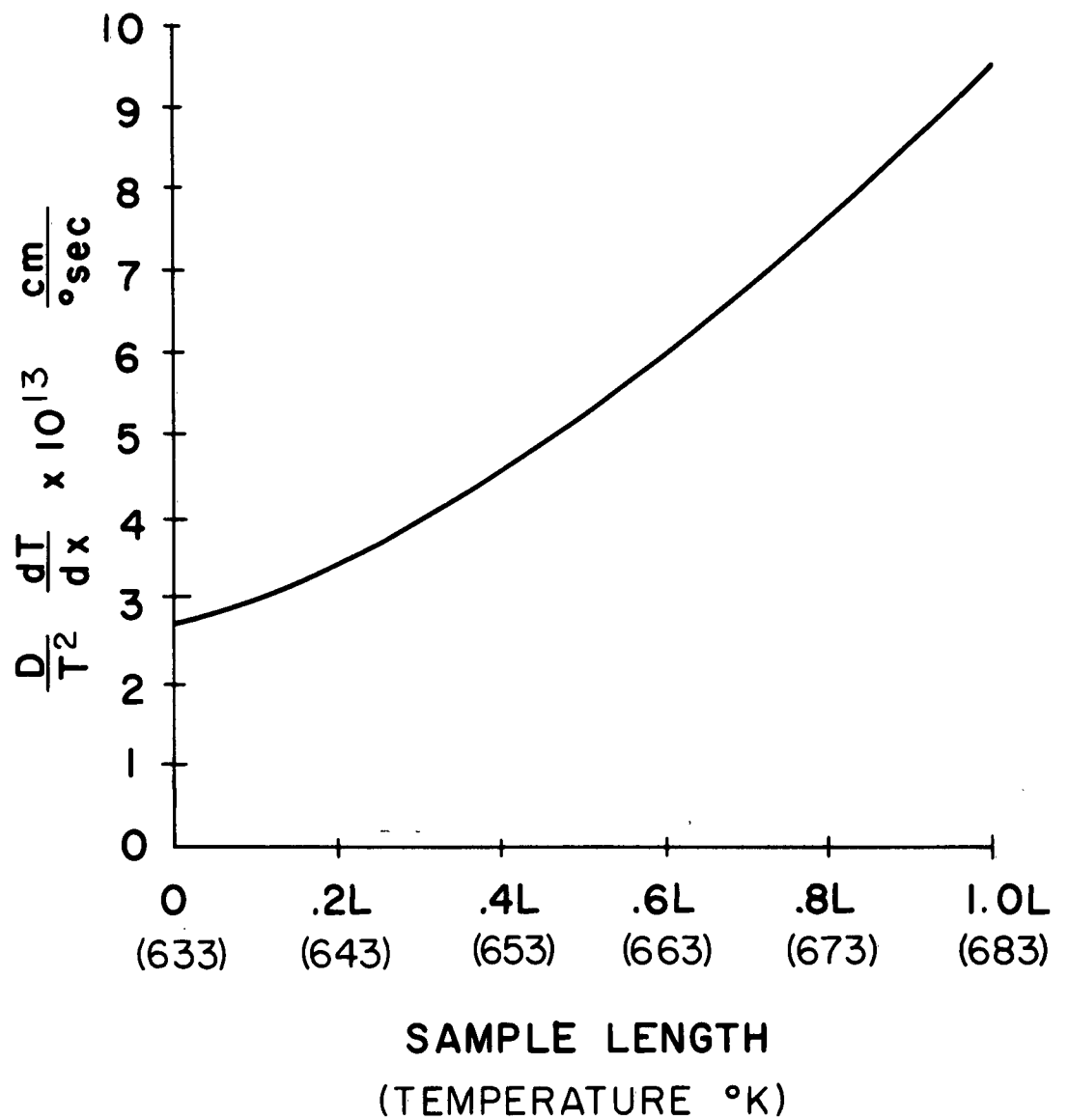
FIGURE 2

III. Thermal Diffusion Apparatus

A. Design of Annealing Apparatus

An important criterion for a thermal diffusion experiment is that a well defined temperature gradient must be established. The main objection to most thermal diffusion experiments to date is the lack of quantitative knowledge about the temperature gradient. Preliminary experiments made in this laboratory indicated that it is possible to observe a minimum in a plot of temperature versus distance along the sample when an apparatus such as that of Shewmon[11] is used.

To circumvent difficulty with the temperature gradient a sample heating arrangement is used which essentially eliminates convection and radiation heat transfer and leaves just conduction as a route for heat to travel through the sample. The apparatus for applying the temperature gradient to thermal diffusion samples is shown in Fig. 3. This figure is self explanatory for the most part. However, the radiation shields require additional explanation.

Convection is eliminated by enclosing the temperature gradient apparatus in a vacuum bell jar and maintaining a pressure equal to about five microns of mercury.

Radiation heat losses from the sample are eliminated by utlization of a series of radiation shields around the sample. The radiation shields around the sample are constructed of a new laminar-type material designated as superinsulation by workers in the cryogenics field. This high efficiency insulation functions

TEMPERATURE GRADIENT APPARATUS
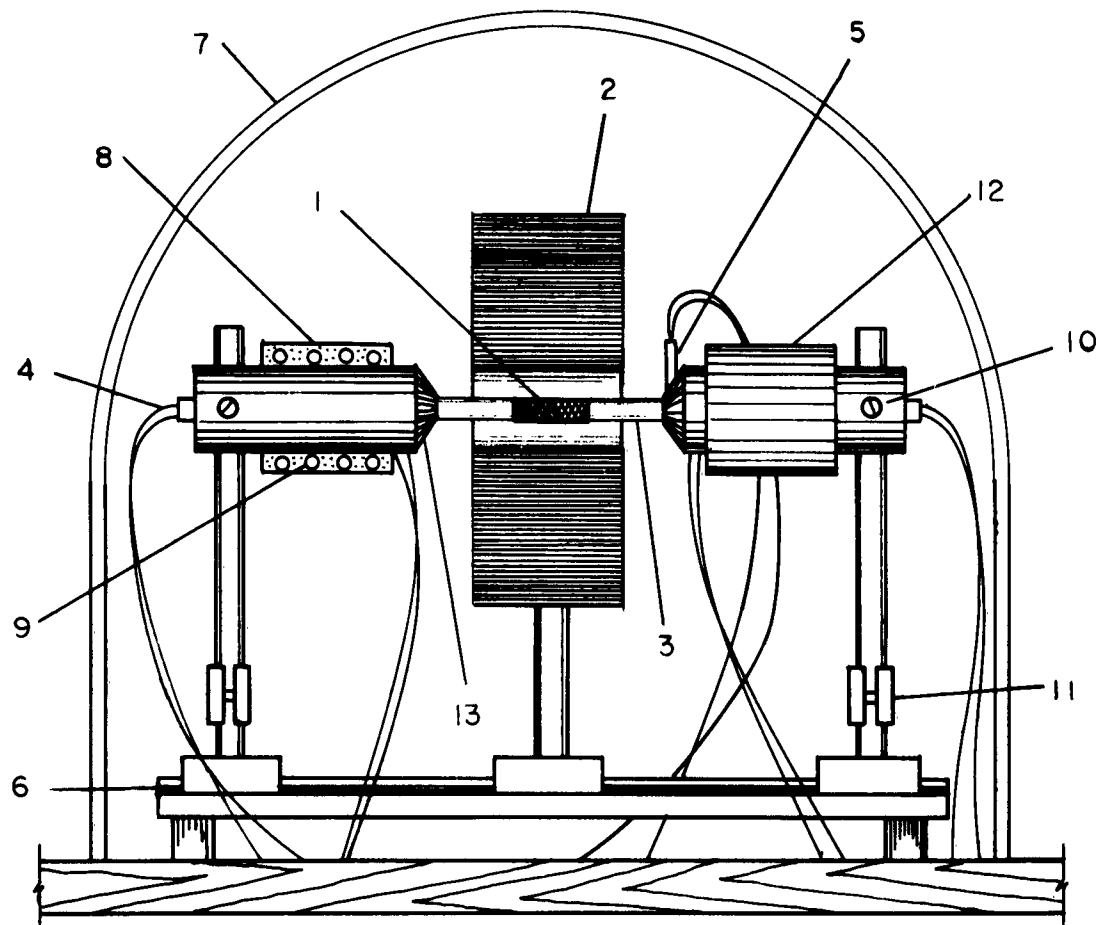
I	SAMPLE MATERIAL	7	VACUUM BELL JAR
2	RADIATION SHIELD-MULTIPLE LAYERS (SHOWN IN SECTION)	8	ALUNDUM CEMENT
3	GRAPHITE HEAT CONDUCTOR WITH MEASURING THERMOCOUPLE	9	RESISTANCE HEATING WIRES
4	MEASURING THERMOCOUPLE WIRES	10	ADJUSTING SCREWS
5	CONTROL THERMOCOUPLE	11	GLASS INSULATOR
6	TONGUE & GROOVE ALLIGNMENT	12	HEATING JACKET
		13	COPPER CORE

FIGURE 3

to simultaneously reduce conduction, convection, and radiation heat
transfer in the direction perpendicular to the plane of the layers
of materials which are built up into the structure designated as
superinsulation.

Superinsulation[27] consists of a multilayered sandwich of
a bright highly reflective substance separated by a spacer material
of low thermal conductivity. The metal foil used in the radiation
shield shown in Fig. 3 is of the nichrome composition (60 per cent
nickel and 16 per cent chromium) and is 0.001 inch thick. The
spacer material is a mica paper manufactured by the Minnesota Mining
and Manufacturing Company and is 0.005 inch thick.

Dimensionally the radiation shield complex has an inside
diameter of 5mm, an outside diameter of 146mm and is 65mm long.
There are approximately 460 double layers of mica paper and
nichrome foil in the set of radiation shields.

Heat which is radiated from a hot to a cold surface is
directly proportional to the emissivity of the surfaces and is
inversely proportional to the number of surfaces or shields. Thus,
to cut radiation losses, a large number of shields with low emissivity
are needed. Material such as nichrome foil has an emissivity of
0.10 (90 per cent of incident radiant heat is reflected) and is there-
fore a very effective block to radiant heat transfer. This is
especially true since 460 double layers comprise the radiation shield.

Gaseous conduction between layers of superinsulation is minimized
because the spacing between layers of insulation is less than the mean

free path of the gas molecules present in the evacuated environment. Thus the heat conducted through the residual gas present is directly proportional to the gas pressure.

The amount of heat conducted through the spacer material is directly proportional to the thermal conductivity of the material and to the conductivity heat flow in areas of contact between particles. Low heat conduction in the spacer material is dependent upon low conductivity of the material itself, the size and geometry of the fibers contained in the material, and the presence of discontinuity in the fibers.

Barron[27] reports on the characteristics of different superinsulations which have been measured. The superinsulation comprising the radiation shield shown in Fig. 3 is closest in properties to the one described in Barron's article which utilizes 0.001 inch aluminum foil and 0.005 inch fiberglass as an insulating material. He reports this material to have a thermal conductivity of 4.9×10^{-5} Btu/hr.-ft.-dog.F. This is measured under conditions of higher vacuum than the present apparatus and the aluminum foil he used has slightly lower emissivity characteristics than the Nichrome foil used here (0.05 versus 0.10). Bearing these uncertainties in mind it would be a conservative estimate to state than the Nichrome-mica paper superinsulating radiation shield employed in this investigation has a conductivity below 10^{-3} Btu/hr.-ft.-deg.F.

Calculations are made which show that radiation heat losses from the sample in the radial direction are small with respect to the

amount of heat conducted through the sample due to temperature gradient. One case for which calculations were done shows the radial radiation heat loss to be only 1.7 per cent of the heat conducted along the long axis of the sample. This calculation is based upon a conservative estimate of the total "conductivity" of the super radiation shield.

The purpose of the super radiation shield is to eliminate radial heat losses and thus yield approximately a linear temperature gradient in the case of crystals which have thermal conductivity which changes slowly as a function of temperature. Most metallic crystals fulfill this condition.

The test of whether or not the radiation shields discussed effectively eliminate radiant heat losses from the sample and thereby produce a linear temperature gradient in the sample is of course to actually measure the temperature profile of the sample as it is being heated in a temperature gradient and at the same time is surrounded by the radiation shields.

Proof of the eventual linearity of the temperature gradient in the thermal diffusion sample is established by measuring the temperatures of the two end thermocouples and the one thermocouple which is placed more centrally on the sample. Measurements are taken as a function of time using the mean temperatures of $300°C$ and $400°C$ and temperature gradients of $20°C$, $40°C$, and $60°C$ and positions of the sample thermocouple at the low temperature quarter point, the central or half point, and the high temperature third point. A typical example of these data is shown in Fig. 4. The temperature
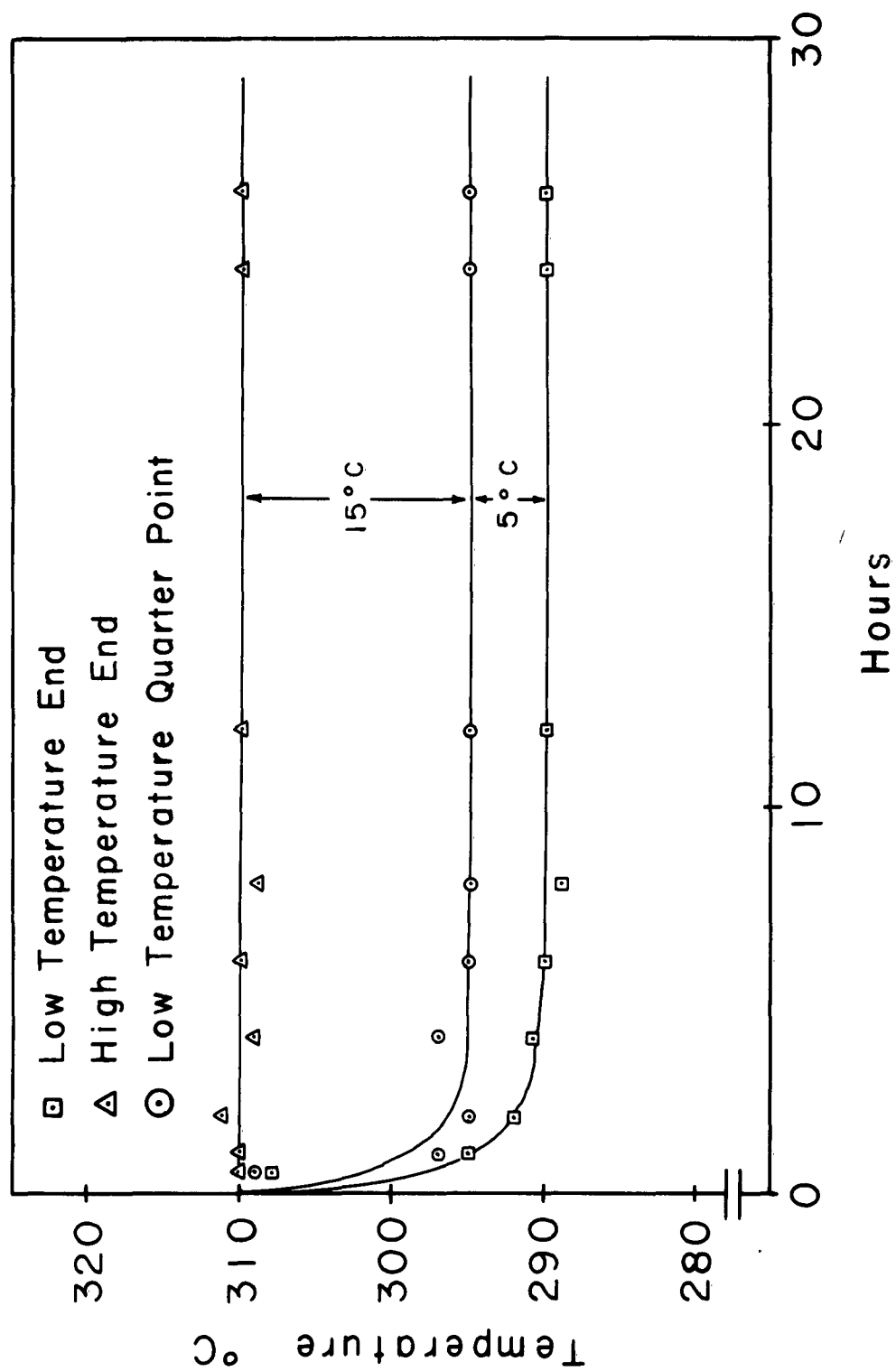
TEMPERATURE PROFILE OF ZINC SPECIMEN

□ Low Temperature End
△ High Temperature End
⊙ Low Temperature Quarter Point

15°C

5°C

Hours

FIGURE 4

Temperature °C

gradient does become linear in the samples measured after a period
of eight to twelve hours.

There is a relatively high inherent inaccuracy in measurements
of this type and there are many valid criticisms which may be applied
to this method of measuring the temperature profile of a solid sample.

The readings of three Pt-Pt 10 per cent Rh thermocouples are
utilized to measure the temperature profile of a zinc sample
surrounded by the radiation shields. These thermocouples are
calibrated against a U. S. Bureau of Standards standard thermocouple
by placing the beads of all three thermocouples in close proximity
in a copper block heated in a tube furnace which is in thermal
equilibrium. The thermocouples are calibrated every 50°C. The
positions of the two end thermocouples are shown in Fig. 3. These
thermocouples are imbedded in the ends of graphite heat conduction
rods shown in the figure. They are actually 0.002 inch inside the
end face of the graphite. A third thermocouple is placed so as to
be as integral a part of the sample to be measured as possible.
The bead is imbedded in a hole in the 3mm x 3mm x 10mm zinc sample
and subsequently the sides of the hole are pushed in over the bead
to mechanically lock the bead in place. This technique allows good
contact between the thermocouple

bead and sample and at the same time presents the bead as an integral part of the sample. Small thermocouple wires 0.005 inch in diameter are used in order that the heat losses down the thermcouples wires be small.

The measurement of the linearity of the temperature gradient in the thermal diffusion samples is really an indication of the effectiveness of the radiation shielding around the sample. When a specimen is placed in the heating arrangement, a slight compressive stress is needed to hold the sample between the graphite heat conducting rods. This compressive stress combined with the high temperature results in stress induced creep, which causes the marker indentions to move closer together thereby masking marker movement due to thermal diffusion.

Creep of this sort is eliminated by replacing the 3mm x 3mm x 10mm sample by a 2mm x 2mm x 10mm sample surrounded by a quartz tube of 3mm I.D., 5.2mm O.D. x 10.050mm long. This arrangement allows the quartz to absorb the compressive stress of the graphite heat conductors. The difference in expansion coefficients of quartz and zinc allows the zinc to expand within the quartz tube due to the temperature rise and just touch the graphite heat conducting rods when the thermal diffusion temperature profile is reached.

Verification of the linearity of the temperature/in the one type of sample heating arrangement described is now extended to the actual case being used; i.e. that of smaller cross section sample closely associated with a quartz tube.

Appendix I shows that for conditions of pure conduction heat transfer, which exists in the thermal diffusion heating apparatus of Fig. 3 the displacement of either the zinc or quartz temperature profiles from linearity due to the temperature coefficient of conductivity is less than $\pm 0.5°C$. The zinc temperature profile deviates in a negative fashion from linearity less than $-0.5°C$ at the maximum displacement and the quartz profile deviates in a positive manner less than $+ 0.5°C$ at the maximum displacement. This means that the temperature profile of the composite zinc sample plus quartz tube must be linear with limits of $\pm .5°C$ at the maximum displacement due to the temperature coefficient of conductivity. The quartz tube in contact with the zinc sample forces the zinc temperature profile to be more linear than if the zinc were present and the quartz tube were not. This effect is due to the opposing signs of the temperature coefficients of conductivity for zinc and quartz.

B. Temperature Control Apparatus

The temperature gradient for the thermal diffusion apparatus is controlled by one temperature controller. One control thermocouple placed in the high temperature heater is utilized. The temperature gradient is controlled by a division of the controller's voltage output into parallel and subsequently reducing one of the parallel voltages through a variable resistor before applying both of these resulting voltages to the non-inductively wound resistance heaters. The temperature control and measuring scheme is shown in Fig. 5.
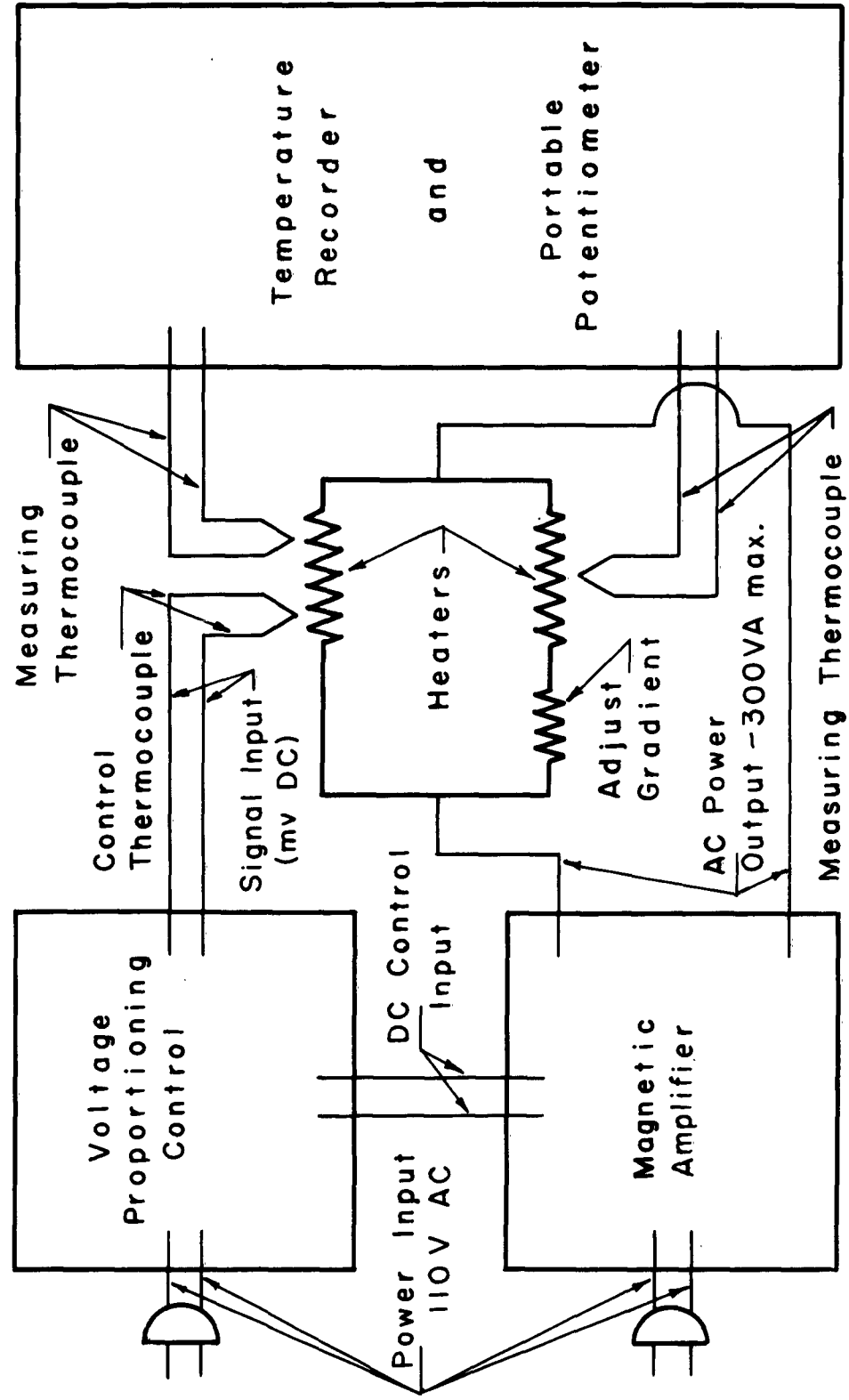
SCHEMATIC OF TEMPERATURE GRADIENT CONTROL

FIGURE 5

The controller used is a Minneapolis-Honeywell Model 106 R 12 voltage proportioning controller, and is a galvanometer calibrated in terms of a variable thermocouple voltage input. The voltage proportioning controller gives continuous indication of the value of the input voltage in terms of a temperature scale and produces an output current proportional to the deviation of the indicating pointer within the adjustable proportional band from the desired control (set) point.

The calibrated accuracy of the controller is designed to be $\pm$ 3/4 per cent of full scale (equivalent to $\pm 4.5°C$). The proportional band is that range of temperature around the set point in which the controller is neither at zero per cent or one hundred per cent output but is somewhere in between. This band is adjustable from 3/4 of 1 per cent to 5 per cent of full scale or from 4°C to 30°C. The output voltage of the controller is amplified to a maximum of 85 volts ac with a Minneapolis-Honeywell 365235-4 magnetic amplifier of 300 volt-amp power output capacity. This is ample power to operate the thermal diffusion apparatus to a temperature of over 600°C.

The output of the magnetic amplifier is then passed through a variable autotransformer, metered (both amps and volts) and divided into parallel. One part of the parallel currents is passed through a variable resistor to control the magnitude of the temperature gradient, and finally the resulting current is passed through the heaters.

The temperatures at the ends of the sample are measured with the above mentioned calibrated Pt-Pt-10 per cent Rh thermocouples running through the heater core and graphite heat conductors.

The performance of the temperature controller can be measured by observing the measuring thermocouple temperatures as a function of time. It is important to know the fluctuations in mean temperature as well as the fluctuations in the magnitude of the temperature gradient. A study of the end temperatures as a function of time reveals fluctuations in the control of the end temperatures of $\pm0.6°C$ and a fluctuation in the control of the magnitude of the temperature gradient of $\pm0.4°C$. The general design of the temperature control arrangement suggests that this arrangement is more suitable for accurately controlling the magnitude of the temperature gradient than it is in controlling the mean or end temperatures. It is possible in principle to reduce the fluctuations in temperature control to $\pm0.1°C$ by narrowing the proportional band on the temperature controller as described above.

Knowledge of the absolute temperature is of course subject to greater uncertainty than the fluctuations in temperature control show. A conservative estimate of the accuracy of knowing the absolute temperatures in the thermal diffusion apparatus would be $\pm6°C$. This estimate is arrived at by considering the various estimated uncertainties associated with temperature measurement in the thermal diffusion apparatus. An uncertainty of $\pm1°C$ is given by the National Bureau of Standards for the Standard thermocouple used in calibrating the thermocouples for the thermal diffusion apparatus. An additional $\pm1°C$ is attributed to errors in the calibration of the apparatus thermocouples. The calibrated thermocouples of the apparatus pass

through the pump plate of the bell jar vacuum system and are then
connected to temperature compensated lead wires which lead to the
temperature recorder and portable potentiometer. This connection is
made by utilizing a short noncompensated copper clip and it is estimated
that an uncertainty of $\pm 1^{\circ}C$ arises because of this situation. The
fact that compensated lead wire is used to carry the thermocouple
emf to the potentiometer plus the fact that a cold juntion compensating
rheostat is used on the potentiometer rather than an ice bath cold
junction results in another estimated $\pm 1^{\circ}C$ uncertainty in the absolute
temperature. An additional $\pm 2^{\circ}C$ uncertainty is added for switching
thermals, the fact that the thermocouples are not calibrated in
position in the thermal diffusion apparatus, the error due to plastic
working of the bead of the thermocouple placed centrally in the sample
during the temperature gradient linearity experiments, and other minor
errors not specifically considered above. These considerations result
in a total estimated uncertainty of $\pm 6^{\circ}C$ for the measurement of the
absolute temperatures in the thermal diffusion apparatus.

C. Marker Producing and Measuring Equipment

The thermal diffusion of vacancies is measured by the
observance of surface marker movement as a function of time during
which the metal sample is subjected to the temperature gradient. Any
marker motion might indicate vacancy flux although surface tension
controlled shape changes must be considered. These will be discussed
later.

Marks were put into the surface of samples of pure zinc by use

of a Tukon hardness testing machine, a Knoop indenter and a 25 gram
load. The markers produced are of an elongated diamond shape and are
placed on all four sides of the specimen at intervals of 0.5mm. The
long axis of the markers are perpendicular to the direction of the
long axis of the sample. The placement of marks on all four sides
of the specimen covering the full length of the sample establishes
a check on sample bending during the temperature gradient anneal.
Identifying marks are also placed on the specimen which identify the
hot and cold ends and also the individual sides.

The distances between marks are also measured by use of a
micrometer eye piece on the Tukon testing machine. A 16mm objective
lens is used in conjunction with a 12.5 x filar eye piece. Under
these circumstances the distance between marks are easily measured
to the nearest filar unit which is equal to 0.735 microns. Measure-
ments of a single distance between any two marker indentions are
reproducable to ± 2 filar units or ± 1.47 microns.

Positions of individual markers relative to all other markers
on a side are measured by utilizing the Microton mechanical stage
of the Tukon testing machine. These positions are read directly
from this mechanical stage to the nearest ten microns and are
estimated to the nearest micron. Reproducability of these readings
is ± 2 microns.

IV. Experimental Technique

The basic technique involves annealing a marked specimen under a temperature gradient for a period of time and subsequently measuring the resulting marker positions as described in Section III.

A. Material Used and Sample Preparation

A pure zinc single crystal of 99.995 per cent purity was obtained from L. Light Company Limited, Polyle Trading Estate, Colnbrook, Bucks, England.

The single crystal is initially cut with a jeweler's saw into pieces 4mm x 4mm x 11mm. It is cut so that the long axis of the sample is parallel to the basal plane of the original zinc single crystal. This cutting process introduces cold work into the samples which must be eliminated prior to the thermal diffusion experiment.

Samples are ground from the original 4mm x 4mm x 1mm dimensions to a size of 2mm x 2mm x 10mm using 400 and 600 grit grinding paper and finally five micron diamond polishing compound. Care is taken during the grinding that very light pressures are utilized so as to minimize additional cold work. The samples are held in a jig during the initial grinding which aids the person preparing the samples in keeping opposite sample faces parallel and in keeping adjacent faces at ninety degrees to each other. A sample which is a rectangular parallelopiped results.

Surfaces are prepared for marking by polishing with five micron diamond polishing compound and subsequently etching in 50 per cent hydrochloric acid. The final step of etching removes much of the cold work in the sample surface which is due to the grinding and polishing operations.

Following the marking procedure described earlier the samples are cleaned by placing them in solutions of detergent, distilled water, and trichloroethane respectively. The samples are encapsulated in a pyrex capsule containing one half atmosphere of dry, purified helium and are subsequently annealed for sixteen hours at 410°C for the purpose of relieving any stresses remaining in the sample.

A quartz tube 3mm I.D., 5.2mm O.D. x 10.1mm is constructed by utilizing a machinist's vee block to align the quartz while grinding to the exact length required. The exact length of quartz tube needed to protect the zinc sample from compressive stress causing creep during the temperature gradient anneal is determined by considering the coefficient of linear expansion of both quartz and zinc and the temperature rise from room temperature to the temperature profile used during the annealing situation. The fact that the length of the quartz tube must be equal to the length of zinc sample when the annealing temperature profile is reached is also a criterion in choosing the relative lengths of zinc and quartz at room temperature. This calculation is shown in Appendix II.

To verify that no compressive stress induced creep takes place during thermal diffusion, the sample and its associated quartz tube are placed in the temperature gradient annealing apparatus and the sample is heated to its normal mean temperature (385°C) under conditions of zero temperature gradient. After twenty-four hours, the sample is removed and the marker positions and distances between markers are measured in the Tukon hardness testing machine. When it

is verified that no stress induced creep is taking place, the sample
and quartz tube are replaced in the temperature gradient annealing
apparatus and the sample is considered ready to undergo the thermal
diffusion annealing treatment.

B. Thermal Diffusion Treatment

A temperature gradient of approximately 50°C/cm with a
mean temperature of 385°C is applied to the zinc sample for
approximately 48 to 72 hours and the sample is subsequently removed
from the apparatus and the distances between marks are measured.
Periods of time such as 48 to 72 hours are utilized for the annealing
treatment because it takes about eight hours for the gradient to
linearize itself as shown in Figure 4. Another reason for this
length of period is due to the fact that the markers move so slowly
that this time is required to detect significant movement. After
measurement, the sample is replaced in the thermal diffusion
apparatus and the cycle is repeated. In this fashion a series of
marker displacements as a function of time is obtained.

Measurement of the markers is accomplished by utilizing the
optical system of the Tukon hardness tester after each temperature
gradient anneal. Both the position of markers relative to each
other and distance between adjacent markers are measured on all sides
of the specimen. The side of the specimen which is undergoing
measurement is also recorded.

C. Final Examination and Verification of Procedure

Creep due to surface tension tends to force the
rectangular parallopiped sample into a spherical shape and also affects

marker positions and distances. This effect is pointed out by Huntington and Ho[30].

The creep due to surface tension may be investigated by annealing the sample in the temperature gradient apparatus under zero temperature gradient and at the mean temperature of the temperature gradient in the thermal diffusion experiment for a period of time of the same order as that required for the thermal diffusion experiment. Measurements of the separation and positions of markers are also made at intervals of 48 to 72 hours during this zero gradient anneal.

Following the heat treatment for thermal diffusion and that for surface tension induced creep, the sample is polished and etched to reveal recrystallization grain size if any recrystallization occurs to the single crystal during the various annealing treatments given during the course of this investigation.

V. Results

The results of two experiments in which marker movement was measured will be presented. The errors involved in these measurements will be indicated.

A. Measurement of Marker Movement

The experimental measurement of marker movement as a function of time is utilized in Equation (40) to calculate the ΔE term of Equation (35) which is related to the heat of transport and to the heat of formation of vacancies in a pure crystal.

The relative displacement of markers placed every 0.5mm along the sample length is measured. The displacements are summed over the length of the sample and the results are averaged over the four faces. These results are presented in Fig. 6 and Fig. 7 as relative marker displacement vs time for two zinc samples.

The slope of the line drawn through the data points using the least squares method is utilized in Equation (40) to calculate ΔE. From the data in Fig. 6 a value of ΔE equal to -8800 cal/mole is obtained. In the second sample shown in Fig. 7 marker movement apparently does not commence immediately but appears to begin after 180 hours of immersion in the thermal gradient. The slope of the line after this time yields a value of ΔE equal to -7520 cal/mole.

It is not clear why marker movement does not occur prior to 180 hours. There is a possibility, however, that the apparent lack of marker movement prior to 180 hours is linked to the fact that the sample was cleaned by ultrasonic methods prior to this time before making marker measurements and was not cleaned ultrasonically after
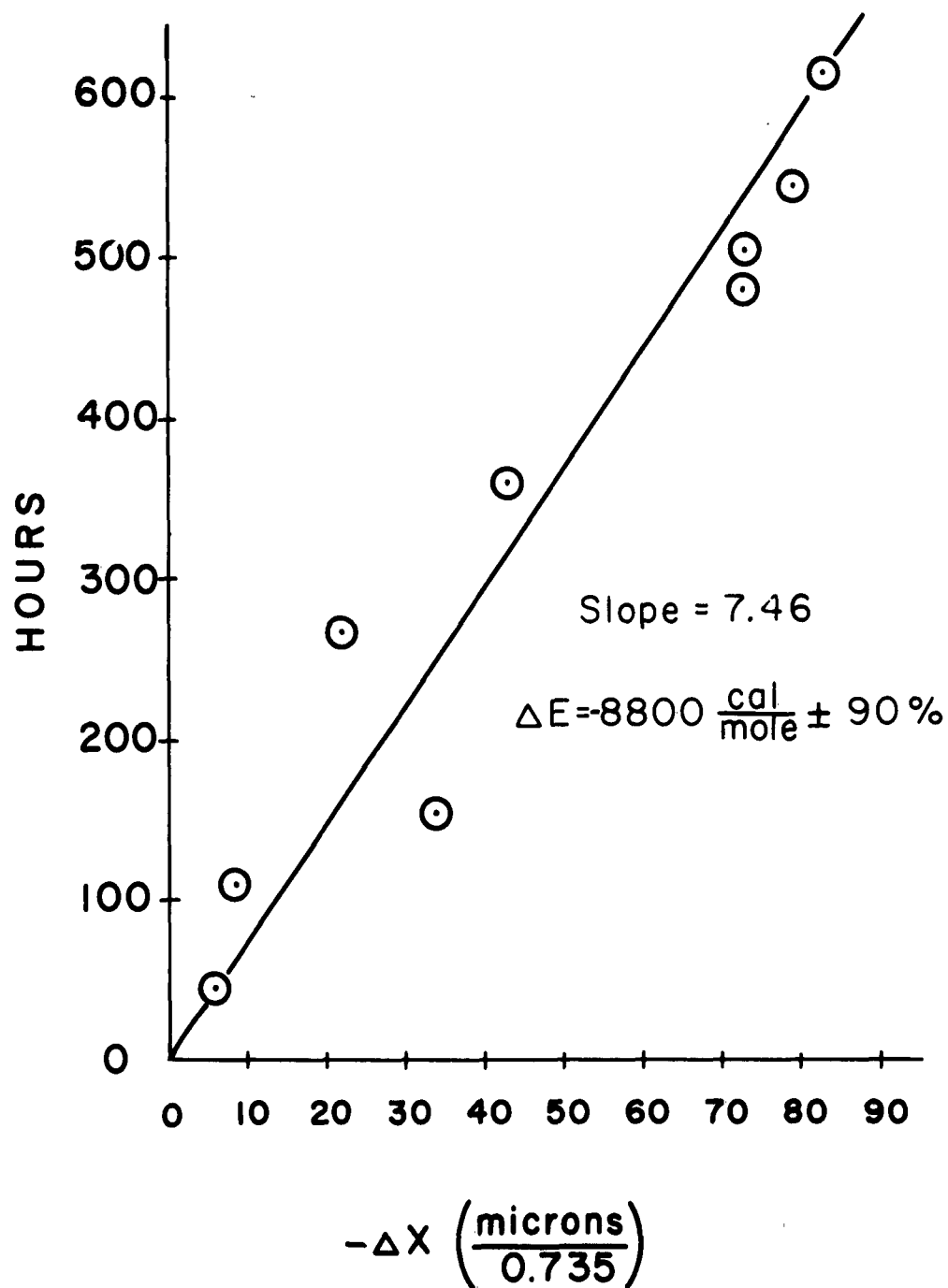
RELATIVE MARKER MOVEMENT vs TIME (Zn #8)

Slope = 7.46

$\Delta E = -8800 \frac{cal}{mole} \pm 90\%$

$-\Delta X \left(\frac{microns}{0.735}\right)$

FIGURE 6

RELATIVE MARKER MOVEMENT
vs TIME (Zn #10)

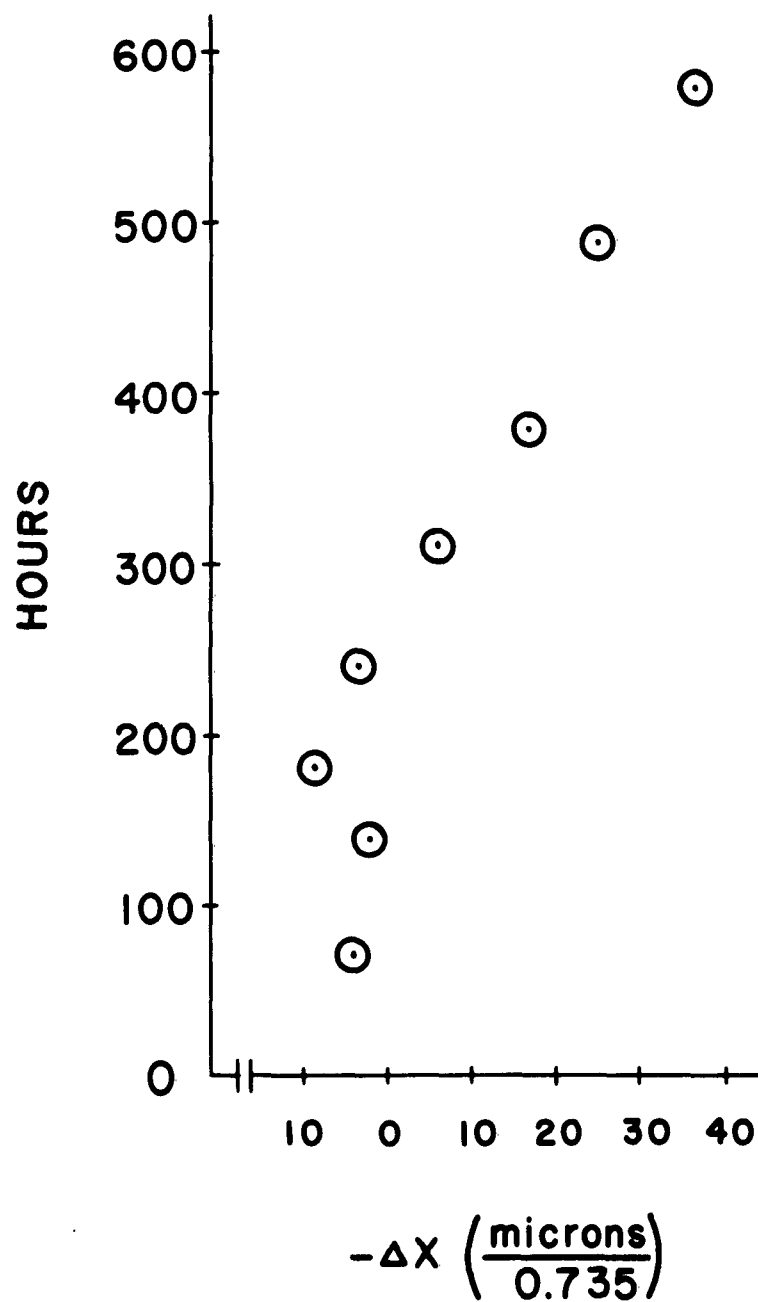FIGURE 7

this time. This factor, however, remains to be investigated experimentally.

B. Errors

Approximate analysis of errors involved in ΔE may be obtained by taking the total differential of Equation (40) and dividing this by Equation (40). This results in the fractional error in ΔE.

$$\frac{\delta \Delta E}{\Delta E} = \frac{\delta \Delta x}{\Delta x} + \frac{\delta t}{t} + \frac{\delta (\frac{dT}{dx})}{(\frac{dT}{dx})} + \frac{(\frac{\Delta H_D}{kT_1} -2)}{\frac{D_{T_2} T_1^{2}}{D_{T_1} T_2^{2}} -1)} \frac{\delta T_1}{T_1} + \frac{(\frac{\Delta H_D}{kT_1} -2)}{\frac{D_{T_1} T_2^{2}}{D_{T_2} T_1^{2}} -1)} \frac{\delta T_2}{T_2} \tag{44}$$

where ΔH_D is the activation barrier for self diffusion.

The fractional error in the relative displacement of markers Δx is taken to be the standard error of the mean point as taken from the scatter of the Δx vs t data in Fig. 6 divided by the average Δx moved per measurement. From this consideration the fractional error is the relative displacement of the markers is

$$\frac{\delta \Delta x}{\Delta x} = 0.25 \tag{45}$$

The fractional error in the time interval is strictly an estimate based upon the time for initiation of the temperature gradient, the time for cooling the sample, the time required to establish the temperature gradient and the average period of application of the temperature gradient between measurements of the relative displacements of the markers. This estimate was taken to be

$$\frac{\delta\, t}{t} = 0.05 \tag{46}$$

in all cases.

The determination of the error in the temperature gradient includes the temperature fluctuations and the uncertainty of knowing the specimen length (this latter effect is negligible). The result of these considerations gives a fractional uncertainty in the temperature gradient of

$$\frac{\delta\left(\frac{dT}{dx}\right)}{\frac{dT}{dx}} = 0.10 \tag{47}$$

The term $\dfrac{\left(\dfrac{\Delta H_D}{kT_1} - 2\right)}{\left(\dfrac{D_{T_2}\, T_1^2}{D_{T_1}\, T_2^2} - 1\right)}$ $\left(\dfrac{\delta\, T_1}{T_1}\right)$ is determined

by assuming $T_1 = 683°K$ and $T_2 = 633°K$ and $\Delta H_D = 24.3k$ cal/mole for self diffusion perpendicular to the hexagonal axis in zinc. The uncertainty in T_1 is taken to be one per cent due to temperature measurement uncertainty plus one per cent due to temperature fluctuations.

Using these parameters:

$$\frac{\left(\dfrac{\Delta H_D}{kT_1} - 2\right)\ \dfrac{\delta\, T_1}{T_1}}{\left(\dfrac{D_{T_2}\, T_1^2}{D_{T_1}\, T_2^2} - 1\right)} = 0.37 \tag{48}$$

and
$$\frac{(\frac{\Delta H_D}{RT_2} -2) \frac{\delta T_2}{T_2}}{(\frac{D_{T_1} T_2^2}{D_{T_2} T_1^2} -1)} = 0.13 \tag{49}$$

The fractional error in the ΔE determination of zinc sample number 8 is obtained by adding relations (45-49) and this results in:

$$\left(\frac{\delta \Delta E}{\Delta E}\right)_{Zn \#8} = \pm 90 \text{ per cent } \Delta E \tag{50}$$

The factor of surface tension induced creep needs to be evaluated. In order to minimize the surface energy of a sample, the specimen will have a tendency to contract in length. Preliminary experiments indicate that this problem is not important in this research but further work must be performed.

VI. Discussion

Although the results of the thermal diffusion program for zinc are not complete, it may be of some interest to examine the nature of the term ΔE. The difference between the kinetic and thermodynamic approaches to the problem of self diffusion in a temperature gradient are disclosed in the derivation and interpretation of the quantity ΔE of Equation 1 or 34. The discussion will be limited to the case where the vacancy mechanism of diffusion dominates and the ΔE considered will be that of Equation 34.

Other investigators have examined ΔE and, because of difference in notation, it is not obvious from a casual view of their work whether or not they obtain consistent results.

The work of Meechan and Lehman[13] agrees with that of Brinkman[18], LeClaire[17] and Brammer[12] who utilize the kinetic approach of Wirtz[14]. Meechan and Lehman also agree with Allnatt and Rice[21] who consider the random walk approach of thermodynamics as a means of examining the problem of thermal diffusion of vacancies in pure metals. In the notation of this paper the above mentioned investigators infer that $\Delta E = \Delta H_m - \Delta H_v$ where ΔH_v is the energy of formation of vacancies.

Shewmon[31] describes the application of the conclusions of Wirtz's general kinetic theory to the case of vacancy diffusion in metals. In this treatment ΔH_m is divided into three energy contributions. Two of these are associated with ΔH_v in the equation for ΔE which results.

The thermodynamic approach is utilized by Shewmon[11] in his paper on the thermal diffusion of vacancies in zinc to show the relation between marker movement and ΔE. He uses the ideas of the kinetic approach to interpret ΔE and concludes that $\Delta E = B\Delta H_m$ and $Q^* = Q_1^* - Q_2^* = B\Delta H_m + \Delta H_v$ where B represents the fraction of ΔH_m which is absorbed by the moving atom at the initial site and is transported to the final site.

It should be pointed out that when considering the thermodynamic approach to the problem of the thermal diffusion of vacancies, certain investigators erroneously define the heat of transport Q_1^* as

$$Q_1^* = \left. \frac{J \text{ energy}}{J_i} \right|_{\text{grad } T=0, \ J_i=0 \ (i \neq j), \ dp=0} \tag{51}$$

where subscripts i and j refer to atoms and vacancies. Physically this definition appears to be incorrect since, when the vacancy mechanism of diffusion is considered, J_j must be non zero in order that J_i may be non zero.

It is derived in the phenomenological theory section of this work that

$$\Delta E = 2Q_2^* - \frac{\Delta H_v}{N_1} \tag{52}$$

For the case of vacancy diffusion in pure metals $N_1 = 1$ and Equation 52 may be reduced to:

$$\Delta E = 2Q_1^* - \Delta H_v \quad \text{where} \quad Q_1^* = -Q_2^* \tag{53}$$

It is noted that $2Q_1^*$ in Equation 52 of this work corresponds to the term ΔH_m in the equation for ΔE implied by the work of Brinkman, LeClaire, Brammer, Allnatt and Rice, and Meechan and Lehman. Thus Q_1^* associated with this work corresponds to one half the energy barrier for atom or vacancy migration as discussed by the above mentioned investigators.

A comparison of the present work regarding Q_1^* with the theoretical kinetic ideas of Shewmon[11] yields the fact that $2Q_1^*$ of the present work corresponds to $B\Delta H_m + \Delta H_v$ of Shewmon.

It is interesting to examine the meaning of Q_1^* of the phenomenological theory presented earlier in this work and subsequently to extrapolate the macroscopic phenomenological result to the atomistic scale. The result of this consideration will be compared with the results of other investigators as presented above in the notation of this work.

The energy flux J_3 is related to the atom and vacancy fluxes through Equation 4 of the theory section:

$$J_3^* = k\delta(\tfrac{1}{T}) + Q_1^* J_1^* + Q_2^* J_2^* \tag{54}$$

It has been shown that

$$J_1 + J_2 = 0 \tag{55}$$

and

$$Q_1^* = -Q_2^* \tag{56}$$

Thus

$$J_3^* = k\delta(\tfrac{1}{T}) + 2Q_1^* J_1 \tag{57}$$

The usual condition applied when considering the heat of transport Q_1^* is that the temperature gradient is zero.

Thus

$$Q_1^* = \left. \frac{J_3^*}{2J_1} \right|_{grad\ T\ =\ 0} \tag{58}$$

An extrapolation from the macroscopic point of view to the atomistic yields the result that Q_1^* represents one half the energy above the average enthalpy, transferred when an atom jumps into a vacant site. Thus $2Q_1^*$ is the total energy transferred over the average enthalpy when an atom-vacancy interchange of position occurs.

An experimental test of the equation implied in the work of Brinkman, LeClaire, Brammer, Allnatt and Rice, and Meechan and Lehman

$$\Delta E = \Delta H_m - \Delta H_v \tag{59}$$

may be made by first noting that

$$\Delta H_D = \Delta H_m + \Delta H_v \tag{60}$$

and combining Equations 59 and 60 to obtain the relation between the experimentally measurable quantities ΔE, ΔH_D, and ΔH_v. The resulting relation is:

$$\Delta E = \Delta H_D - 2\Delta H_v \tag{61}$$

A careful experimental determination of the three quantities in Equation 61 would constitute an experimental test of the validity of Equation 59 which is primarily a result of a kinetic treatment of the thermal diffusion of vacancies in pure metals.

It would seem from the kinetic point of view of Wirtz[14] or from a similar kinetic treatment of Q^* by Shewmon[11] that Q_1^* would be proportional but not equal to ΔH_m although there is no indication

from the formality of this work which of the two is the more appealing kinetic treatment.

If a reasonable value for the heat of formation of vacancies ΔH_v can be assumed then $2Q_1^*$ may be calculated from Equation 53 as

$$2Q_1^* = \Delta E + \Delta H_v \tag{62}$$

Gertsriken and Slyusar[32] present the results of experimental measurements of ΔH_v for pure zinc and also for a group of other pure metals. These determinations were made by the use of both quenched in resistivity and dialatometric methods. The quench method is subject to criticism[33] and some of the results obtained by Gertsriken and Slyusar differ from the results of others by factor of two. The data of Gertsriken and Slyusar are the only data available for ΔH_v in pure zinc but however must be utilized with caution.

By taking the published value of ΔH_v = 8.7 kcal/mole and the result from the first sample of this investigation that ΔE = -8.8 kcal/mole, Q_1^* may be calculated from Equation 62. Thus utilizing the experimental values presented here, $2Q_1^*$ = -.1 kcal/mole. It will be noted, however, that this value must be taken with reservation due to the uncertainty of the ΔE determined in this work and that of ΔH_v determined by Gertsriken and Slyusar.

Shewmon[31] quotes a calculated value for the relation between ΔH_v, ΔH_m and ΔH_D for copper which has a fcc structure. The value for copper

$$\frac{\Delta H_v}{\Delta H_v + \Delta H_m} = 0.60$$

is extended to the case of zinc which has a hop structure and it is estimated on this basis that $\Delta H_v = 14.6$ kcal/mole. If this estimate of ΔH_v is utilized along with the experimental determination of ΔE as presented in this work, the result is that

$$2Q_1^* = +5.4 \text{ kcal/mole.}$$

It is obvious that the value of $2Q_1^*$ is subject to large uncertainty as regards both magnitude and sign. More work must be done to determine both ΔE and ΔH_v to a lower uncertainty before it will be possible to correctly determine the sign of $2Q_1^*$ with any degree of confidence.

VII. Conclusions

Several conclusions may be drawn.

1. An experimental apparatus was constructed which has the capability of yielding a very nearly linear temperature gradient for metal samples.

2. Marker movement does appear to exist in zinc due to the application of a temperature gradient. This differs from past work in other laboratories.

3. ΔE consists of two terms involving the 'heat of transport' and the heat of formation of vacancies:

$$\Delta E = 2Q_1^* - \frac{\Delta H_v}{N_1}$$

where the 'heat of transport' Q_1^* is a defined quantity and represents one half the energy over and above the average enthalpy transferred when an atom makes a jump into a vacant lattice site.

4. ΔE is calculated from preliminary measurements of marker movement and is approximately -8.8 k cal/mole.

5. Additional experiments at constant temperature are needed to determine the effect of surface energy induced creep upon marker movement.

6. The kinetic treatments of the problem of thermal diffusion of vacancies in pure metals lead to the conclusion that, in general, $2Q_1^*$ is related but not equal to ΔH_m.

7. An experimental test of the relation:

$$\Delta E = \Delta H_m - \Delta H_v$$

attributed to investigators Brinkman, LeClaire, Brammer, Allnatt
and Rice, and Meechan and Lehman may be made by accurately measuring
ΔE using a thermal diffusion experiment, ΔH_D using a self
diffusion experiment, and ΔH_V by using resistivity quenching or
dialatometry techniques.

APPENDIX I

Temperature Gradient in Quartz and Zinc

Jakob[28] reports the following thermal conductivities for pure zinc and quartz as a function of temperature:

K_{zn} (Btu/hr ft °F)	T°C
65	0
63	100
61	200
54	400

K_{Quartz} (Btu/hr ft °F)	T°C
.54	-200
.9	-100
1.1	0
1.2	-100
1.3	-200
1.5	-400

From these data it is possible to calculate the temperature coefficient of conductivity for both quartz and zinc from

$$K_T = K_o \left[1 + \alpha \ (T-T_o) \right] \tag{A-1}$$

where K_T is the temperature dependent thermal conductivity, K_o is the thermal conductivity at temperature T_o, α is the temperature coefficient of thermal conductivity and T is the absolute temperature at which K_T is desired. Thus

$$\alpha_{zn} = -0.57 \times 10^{-3} (^\circ)^{-1}, \tag{A-2}$$

and
$$\alpha_{quartz} = 0.83 \times 10^{-3} (^\circ)^{-1} \tag{A-3}$$

It is possible to calculate the temperature profile of a zinc and quartz sample in a temperature gradient. The formula for conduction heat flow is given by Eckert[29] as

$$q = -K_T \frac{dT}{dx}. \tag{A-4}$$

where q is the heat flow per unit area, K is the thermal conductivity and x represents distance. It is known that

$$K_T = K_o \left[1 + \alpha T \right] \tag{A-5}$$

so
$$q = -K_o \left[1 + \alpha T \right] \frac{dT}{dx} \tag{A-6}$$

or
$$\frac{q\,dx}{K_o} = - \left[1 + \alpha T \right] dT . \tag{A-7}$$

Integrating:

$$\frac{q}{K_o} \int_0^x dx = - \int_{T_o}^{T(x)} \left[1 + \alpha T \right] dT \tag{A-8}$$

$$\frac{-qx}{K_o} = T + \frac{\alpha T^2}{2} \Bigg|_{T_o}^{T(x)} \tag{A-9}$$

or

$$\frac{-qx}{K_o} = T(x) - T_o + \frac{\alpha}{2} (T_x^2 - T_o^2) . \tag{A-10}$$

or $\qquad x = -\frac{K_o}{q} \left[\frac{\alpha}{2} T(x)^2 + T(x) - \frac{\alpha}{2} T_o^2 - T_o \right]$ (A-11)

Substituting for q results in:

$$x = \left[\frac{\alpha}{2} T(x)^2 + T(x) - \frac{\alpha}{2} T_o^2 - T_o \right] \frac{1}{\frac{dT}{dx}}$$ (A-12)

It is now possible to set up a table of $T(x)$ vs x for both quartz and zinc by utilizing the above equation.

The α for both quartz and zinc are determined earlier in this appendix. Assuming the temperature gradient to be 50°C from 360°C to 410°C, the following tables result:

Zinc $T(x)$ °K	x	Quartz $T(x)$ °K	x
633	0.000L	633	0.000L
643	0.199L	643	0.199L
653	0.401L	653	0.395L
663	0.603L	663	0.596L
673	0.801L	673	0.797L
683	1.000L	683	1.000L

The temperature profile of zinc should show a negative displacement from a linear gradient and the quartz temperature profile should show a positive displacement from a linear gradient when there exists a condition of pure conduction and no radiation heat transfer. The displacement of the quartz and zinc temperature profiles never exceeds ±0.5°C from linearity when a 50°C gradient exists between the zinc sample and temperatures of 360°C to 410°C.

APPENDIX II

Length of Quartz Protection Tube and Zinc Sample

The equations for linear expansion due to a temperature rise
are

$$L_q = L_{q_o} (1 + \alpha_q T) \qquad (A-13)$$

and

$$L_s = L_{s_o} (1 + \alpha_s T) \qquad (A-14)$$

where L_q is the length of the quartz tube under conditions
of the temperature gradient anneal.

L_{q_o} is the length of the quartz tube at room temperature.

α_q is the linear coefficient of thermal expansion of quartz.

T is the temperature rise above room temperature

L_s is the length of the sample under conditions of the
temperature gradient anneal.

L_{s_o} is the length of the sample at room temperature.

α_s is the linear coefficient of thermal expansion of the
sample.

The condition desired is that $L_s = L_q$ at T

$$L_{q_o} (1 + \alpha_q T) = L_{s_o} (1 + \alpha_s T) \qquad (A-15)$$

or

$$L_{q_o} = \frac{L_{s_o} (1 + \alpha_s T)}{(1 + \alpha_q T)} \qquad (A-16)$$

For a temperature gradient of $360°C - 410°C$, the mean temperature
is $385°C$. This is $360°C$ above room temperature which is taken to

be 25°C. Since $T = 360°C$, $\alpha_q = .546 \times 10^{-6}$ and $\alpha_{zn} = 26.3 \times 10^{-6}$

$$L_{q_o} = 1.01 \ L_{zn_o} \qquad \text{(A-17)}$$

or

$$L_{zn_o} = 99 \text{ per cent } L_{q_o} \qquad \text{(A-18)}$$

It is shown that the quartz tube must be 1 per cent longer than the zinc sample in order that they may both be the same length when the temperature gradient of 360°C - 410°C is applied.

VIII. References

1. K. G. Denbigh: Thermodynamics of the Steady State, Methuen, London (1959).

2. K. Clusius and G. Dickel, Naturwissenschaften 26, 546 (1938).

3. M. Ballay, Rev. Metal 25, 427 509 (1928).

4. T. A. Lebedev, Metallurgy 15, No. 11-12, 61 (1940).

5. L. S. Darken and R. A. Oriani, Acta. Met. 2, 841 (1954).

6. C. Luchock, Senior Thesis, Carnegie Institute of Technology, May 1955.

7. F. Winter and H. G. Drickamer, J. Chem. Phys. 24, 492 (1956).

8. J. Markowitz and J. Belle, WAPD-TM-42, AEC Res. and Dev. Report, Feb. 1957.

9. R. E. Howard, J. Chem. Phys. 27, 1377 (1957).

10. G. D. Rieck and H. A. C. Bruning, Nature 190, 1181 (1961).

11. P. Shewmon, J. Chem. Phys. 29, 1032 (1958).

12. W. G. Brammer, Acta. Met. 8, 630 (1960).

13. C. J. Meechan and G. W. Lehman, J. App. Phys. 33, 634 (1962).

14. K. Wirtz, Z. Physik. 44, 221 (1943).

15. S. R. DeGroot: Thermodynamics of Irreversible Processes, Interscience, New York (1951).

16. W. Shockley, Phys. Rev. 91, 1563 (1953).

17. A. D. LeClaire, Phys. Rev. 93, 344 (1954).

18. J. A. Brinkman, Phys. Rev. 93, 345 (1954).

19. W. Shockley, Phys. Rev. 93, 345 (1954).

20. R. E. Howard and J. R. Manning, J. Chem. Phys. 36 910 (1962).

21. A. R. Allnatt and S. A. Rice, J. Chem. Phys. 33 573 (1960).

22. R. A. Oriani, Thermodynamic Properties of Solids, Liquids, and Gases, American Society of Mechanical Engineers, New York (1959) Monograph.

23. D. O. Raleigh, and A. W. Sommer, J. Chem. Phys. <u>36</u>, 381 (1962).

24. R. A. Oriani, Research Report No. 892, Edgar C. Bain Laboratory, U.S. Steel Corporation (1960).

25. W. G. Brammer, Bul. Am. Phys. Soc. <u>2</u>, 388 (1957).

26. R. O. Davies, Rpts. Prog. in Phys. <u>19</u>, 341-348 (1956).

27. R. F. Barron, Machine Design <u>33</u>, 117 (1961).

28. M. Jakob, <u>Heat Transfer</u>, Wiley, New York (1949).

29. E. R. G. Eckert, <u>Heat and Mass Transfer</u>, McGraw-Hill New York (1949).

30. H. R. Huntington and S. C. Ho, <u>Electromigration in Metals</u>, Preprint, Rensselaer Polytechnic Institute, Troy, New York.

31. P. G. Shewmon: <u>Diffusion in Solids</u>, McGraw-Hill, New York (1963).

32. S. D. Gertsriken and B. F. Slyusar, Fiz. Metal. Metallovod. <u>6</u>, No. 6, 1061 (1959).

33. I.F. Nicholas, Acta. Met. <u>3</u> 411 (1955).

LIST OF FIGURES